

# **Luminescent Citrate-Functionalized Terbium-Substituted Carbonated Apatite Nanomaterials: Structural Aspects, Sensitized Luminescence, Cytocompatibility, and Cell Uptake Imaging**

**Jaime Gómez-Morales <sup>1,\*</sup>, Raquel Fernández-Penas <sup>1</sup>, Francisco Javier Acebedo-Martínez <sup>1</sup>, Ismael Romero-Castillo <sup>1</sup>, Cristóbal Verdugo-Escamilla <sup>1</sup>, Duane Choquesillo-Lazarte <sup>1</sup>, Lorenzo Degli Esposti <sup>2</sup>, Yaiza Jiménez-Martínez <sup>3</sup>, Jorge Fernando Fernández-Sánchez <sup>4</sup>, Michele Iafisco <sup>2</sup> and Houria Boulaiz <sup>3</sup>**

<sup>1</sup> Laboratorio de Estudios Cristalográficos. IACT-CSIC-UGR. Avda. Las Palmeras, n° 4. 18100 Armilla, Spain; raquel@lec.csic.es (R.F.-P.); j.acebedo@csic.es (F.J.A.-M.); ismaelrc92@gmail.com (I.R.-C.); cristobal.verdugo@csic.es (C.V.-E.); duane.choquesillo@csic.es (D.C.-L.)

<sup>2</sup> Institute of Science and Technology for Ceramics (ISTEC), National Research Council (CNR), Via Granarolo 64, 48018 Faenza, Italy; lorenzo.degliesti@istec.cnr.it (L.D.E.); michele.iafisco@istec.cnr.it (M.I.)

<sup>3</sup> Instituto de Biopatología y Medicina Regenerativa (IBIMER), Universidad de Granada, 18016 Granada, Spain; yajimartinez@correo.ugr.es (Y.J.-M.); hboulaiz@ugr.es (H.B.)

<sup>4</sup> Department of Analytical Chemistry, Faculty of Sciences, University of Granada, Avda. Fuentenueva s/n, 18071 Granada, Spain; jffernan@ugr.es

\* Correspondence: jaime@lec.csic.es; Tel.: +34-958525020 or +34-958230000 (ext. 436640)

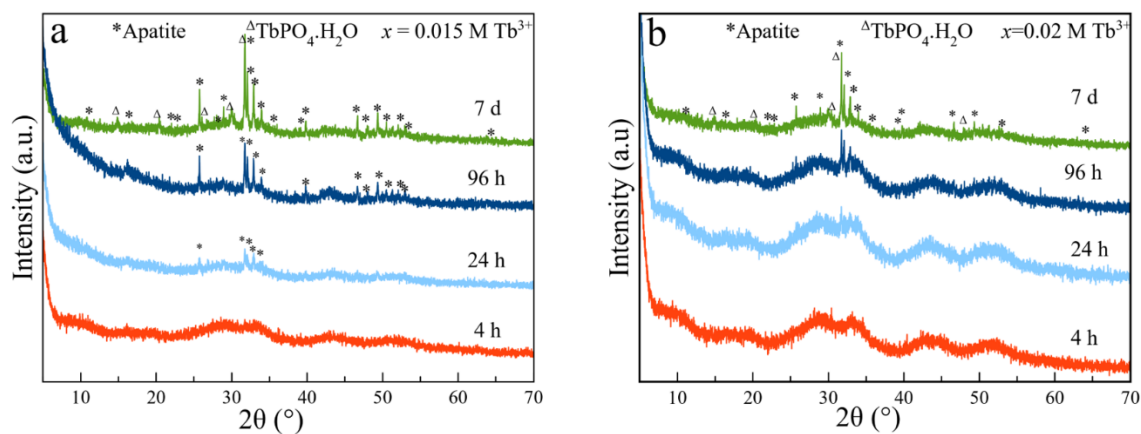


**Figure S1.** XRD diagrams of samples precipitated at 4, 24, 96 and 7 days at Tb<sup>3+</sup>doping concentrations: (a)  $x = 0.015$  M; (b)  $x = 0.020$  M. \* (Apatite phase, PDF 01-1008).  $\Delta$  (TbPO<sub>4</sub>·H<sub>2</sub>O phase, PDF 20-1244).

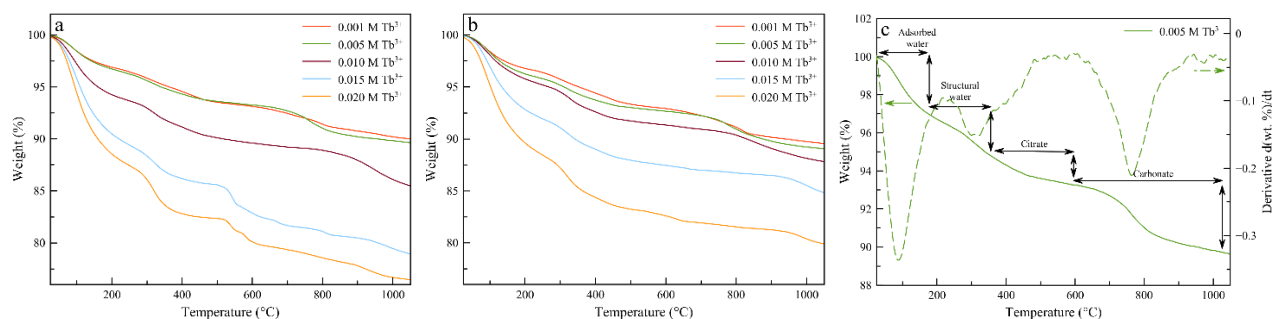


**Figure S2.** TGA curves of samples prepared at (a) 96 h or (b) 7 days of maturation. (c) Representative TGA with DTG curve of 0.005 M Tb<sup>3+</sup> sample with interpretation of mass losses.

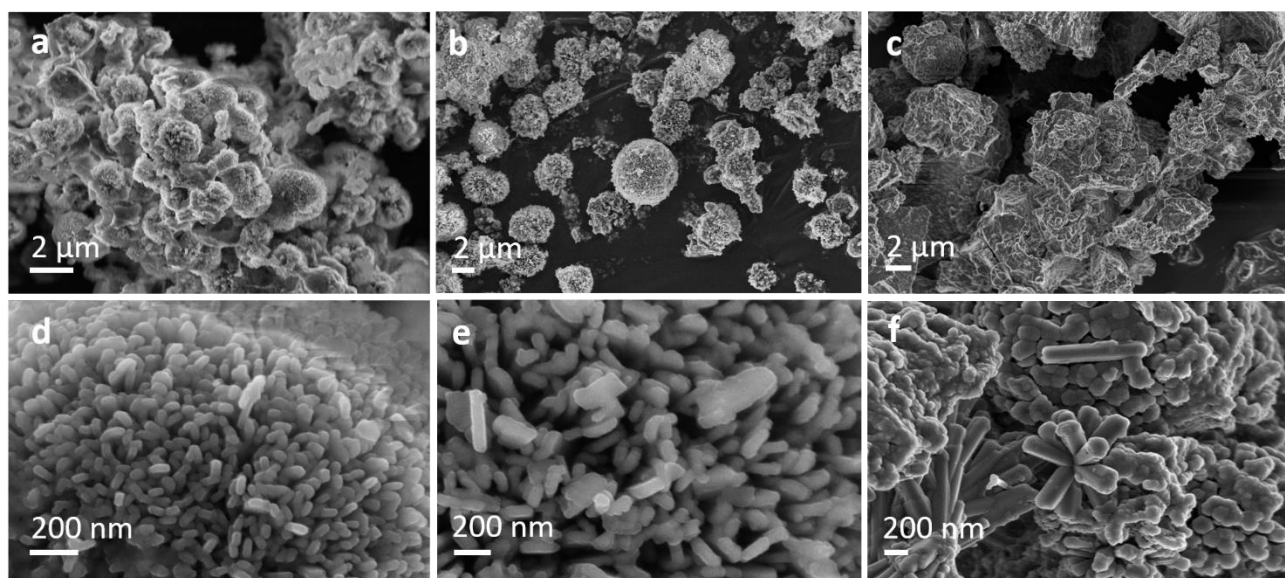


**Figure S3.** FESEM micrographs of samples at 7 days of maturation at  $\text{Tb}^{3+}$  doping concentration of: (a,d)  $x = 0.005 \text{ M}$ ; (b,e)  $x = 0.010 \text{ M}$ , and (c,f)  $0.015 \text{ M}$

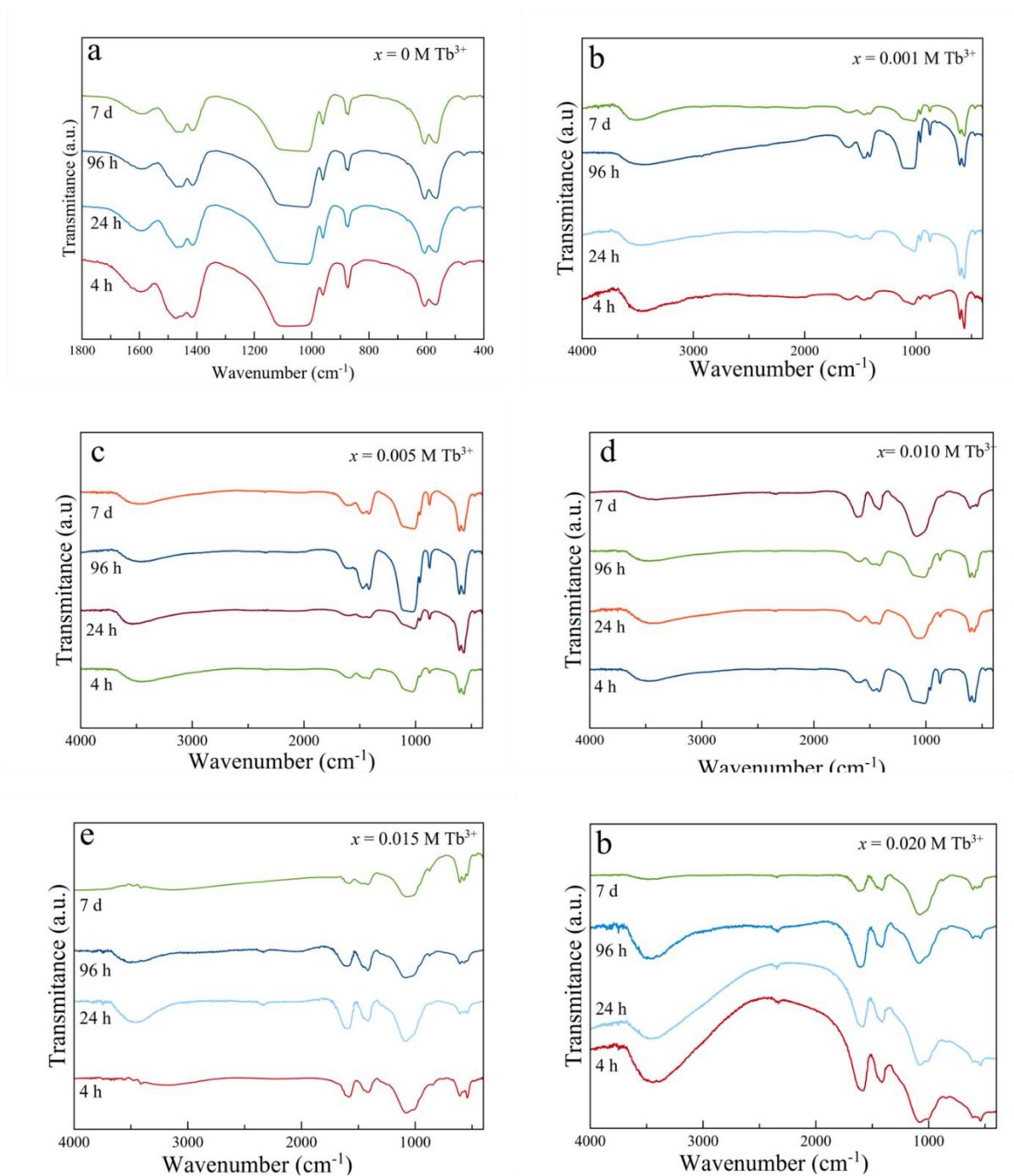


**Figure S4.** FTIR spectra of samples precipitated at 4 h, 24 h, 96 h and 7 days at Tb<sup>3+</sup> doping concentrations of (a)  $x = 0$ ; (b)  $x = 0.001$  M; (c)  $x = 0.005$  M, (d)  $x = 0.010$  M; (e)  $x = 0.015$  M, and (f)  $x = 0.020$  M.

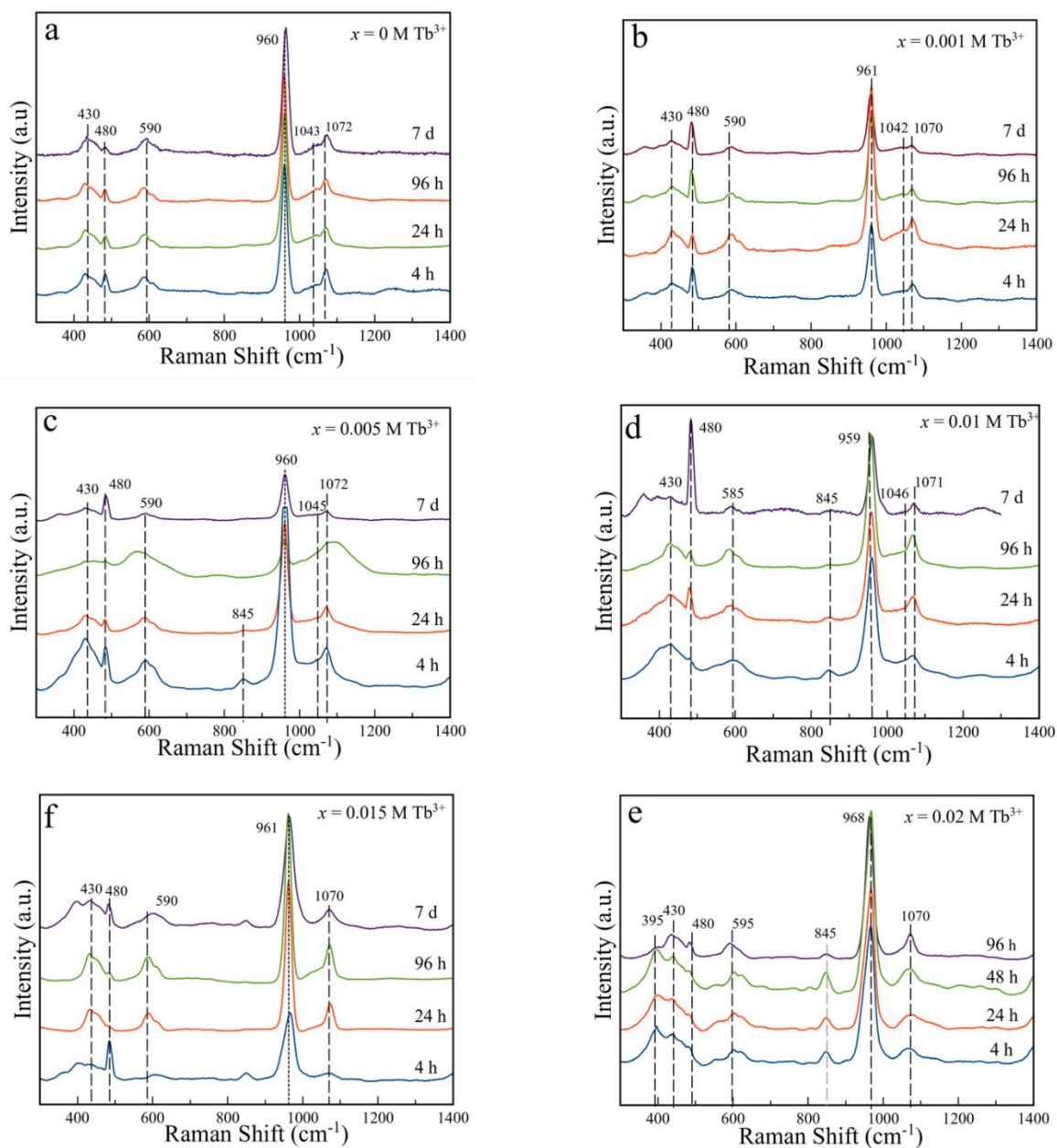


**Figure S5.** Evolution of Raman spectra in function of maturation time of samples with  $\text{Tb}^{3+}$  doping concentrations of (a)  $x = 0$ ; (b)  $x = 0.001 \text{ M}$ ; (c)  $x = 0.005 \text{ M}$  and (d)  $x = 0.010 \text{ M}$ ; (e)  $x = 0.015 \text{ M}$ , and (f)  $x = 0.02 \text{ M}$ .

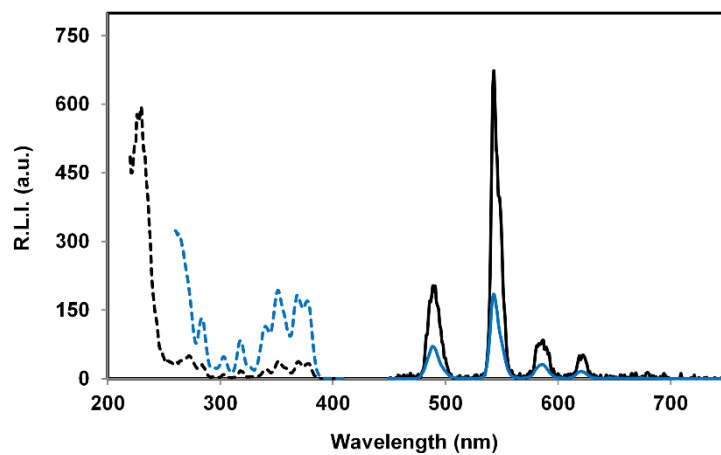


**Figure S6.** Uncorrected excitation (dashed lines) and emission (solid lines) spectra of samples prepared with  $x = 0.02$  M  $\text{Tb}^{3+}$  at maturation time of 96 h using  $t_d = 120 \mu\text{s}$ ,  $t_d = 5\text{ms}$  and a)  $\lambda_{\text{exc/em}} = 230/545$  nm, slit width $_{\text{exc/em}} = 2.5/2.5$  nm, detector voltage 545 v; (b)  $\lambda_{\text{exc/em}} = 375/545$  nm, slit width $_{\text{exc/em}} = 5/5$  nm, detector voltage 470 v.

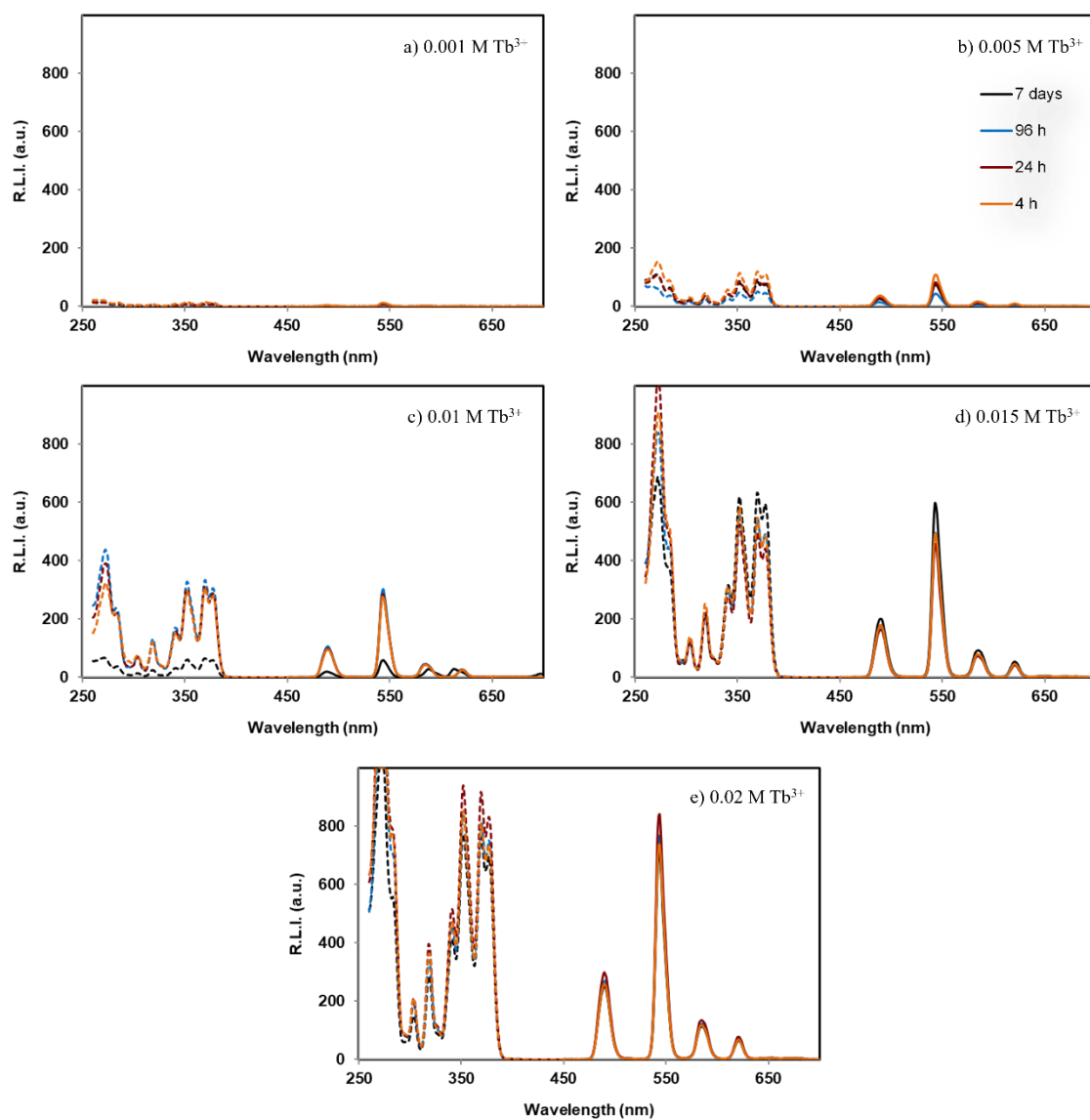


**Figure S7.** Uncorrected excitation (dashed lines) and emission (solid lines) spectra of solid  $\text{Tb}^{3+}$ : cit-cAp samples prepared with different  $\text{Tb}^{3+}$  doping concentration at maturation times of 4h, 24h, 96 h and 7 days.

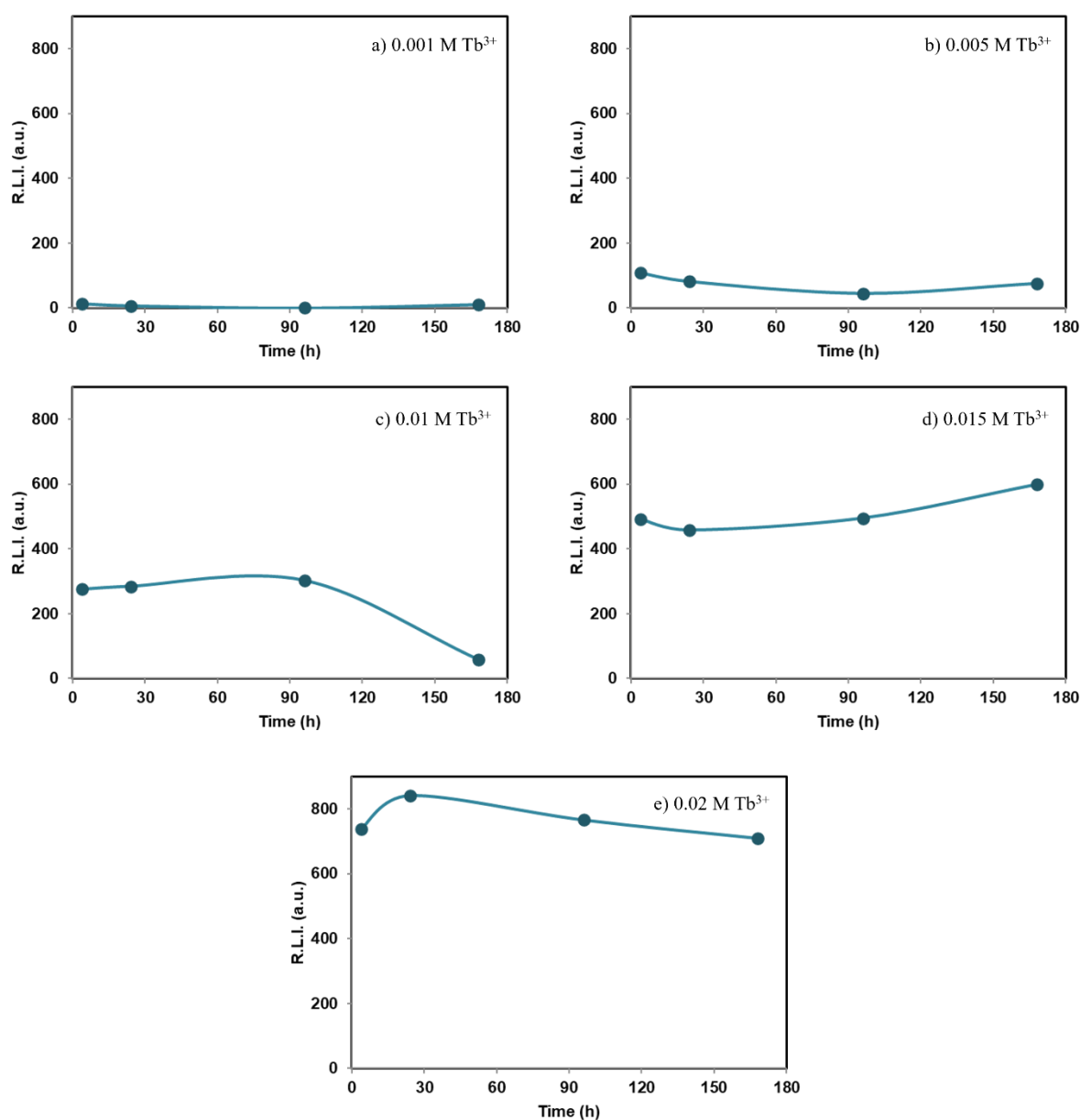


**Figure S8.** Variation of the R.L.I. in function of maturation time of the  $\text{Tb}^{3+}$ :cit-cAp samples at the maximum excitation and emission wavelengths prepared at several  $\text{Tb}^{3+}$  doping concentrations.



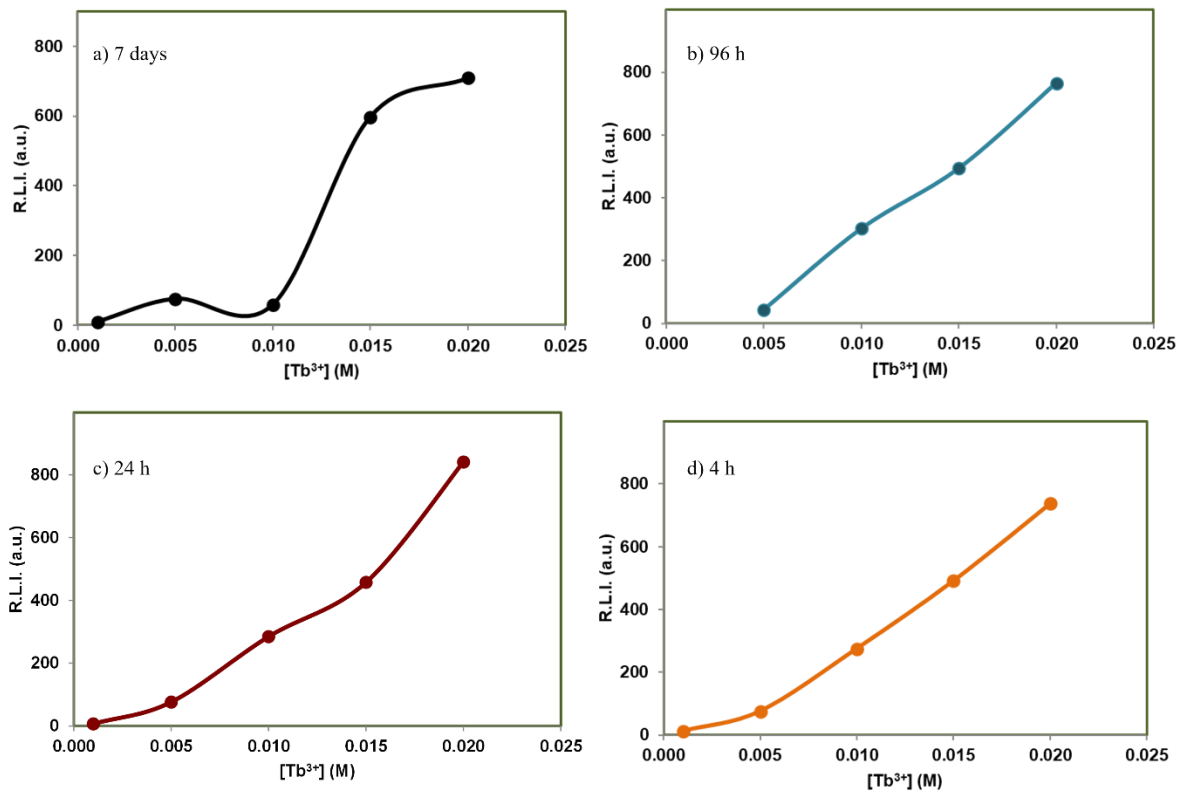


**Figure S9.** Variation of the R.L.I. in function of  $\text{Tb}^{3+}$  doping concentration of the  $\text{Tb}^{3+}$ :cit-cAp samples at the maximum excitation and emission wavelengths at several maturation times.

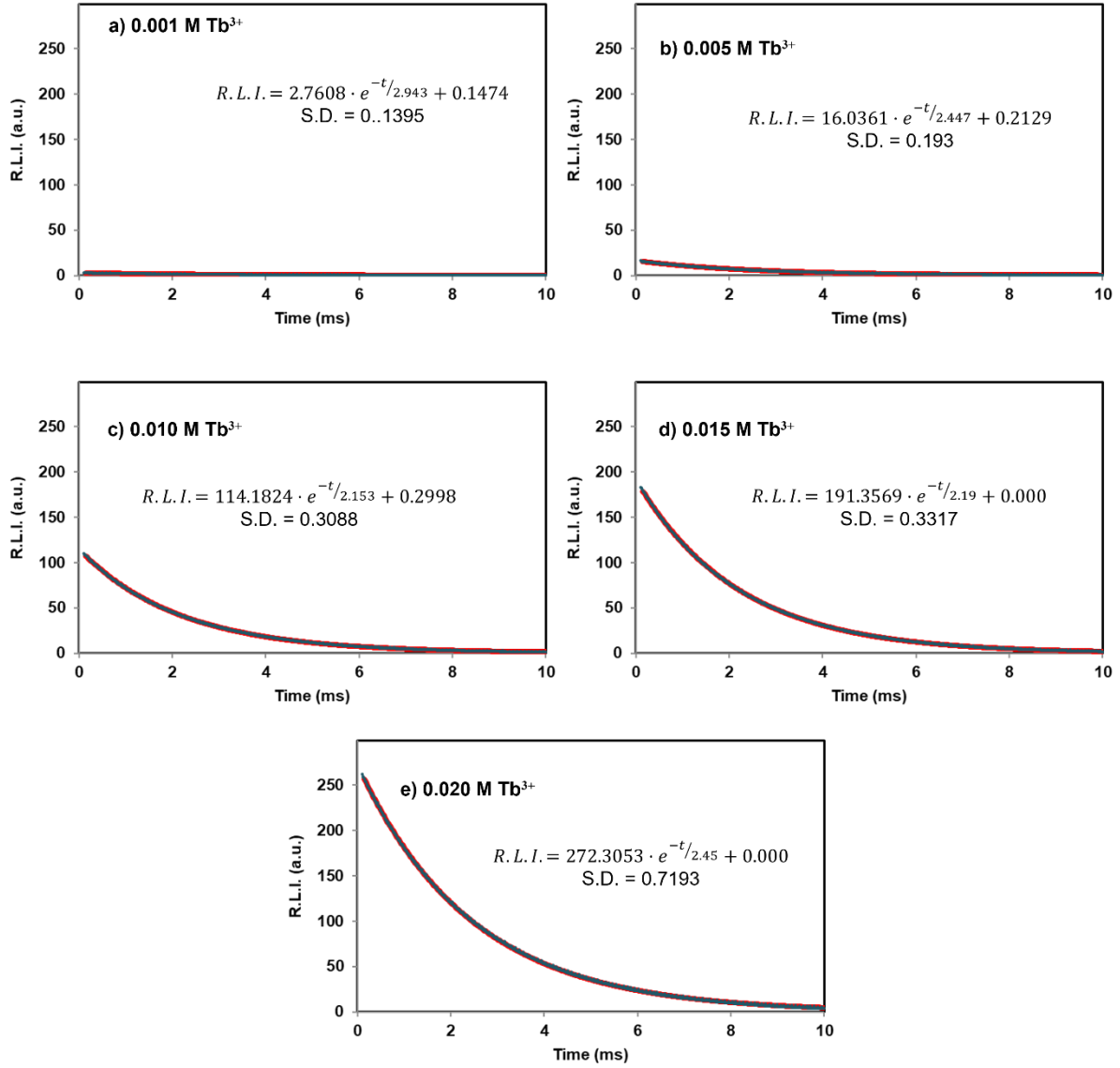


**Figure S10.** Luminescence decay curve of different Tb<sup>3+</sup>:cit-cAp samples at maturation times of 96h,  $t_d = 100 \mu s$ ,  $t_g = 0.01 ms$ ,  $\lambda_{exc/em} = 375/545 nm$ , slit-widths<sub>exc/em</sub> = 10/10 nm, and detector voltage = 600 V. Circles correspond to experimental data (100 cycles) and lines to the fitting equation.

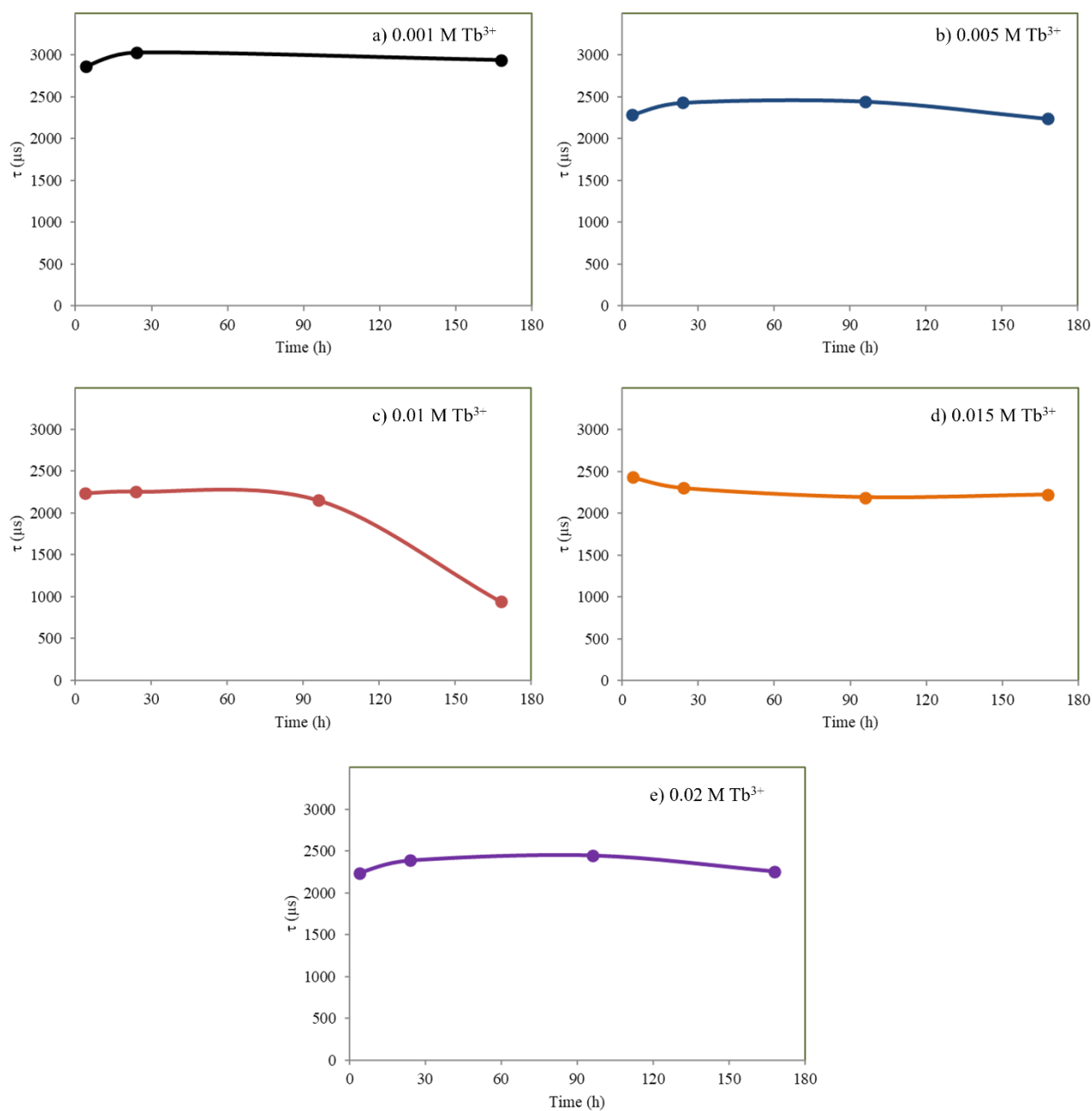


**Figure S11.** Variation of the luminescence lifetime in function of maturation time of the  $\text{Tb}^{3+}$ :cit-cAp samples prepared at several  $\text{Tb}^{3+}$  doping concentrations.

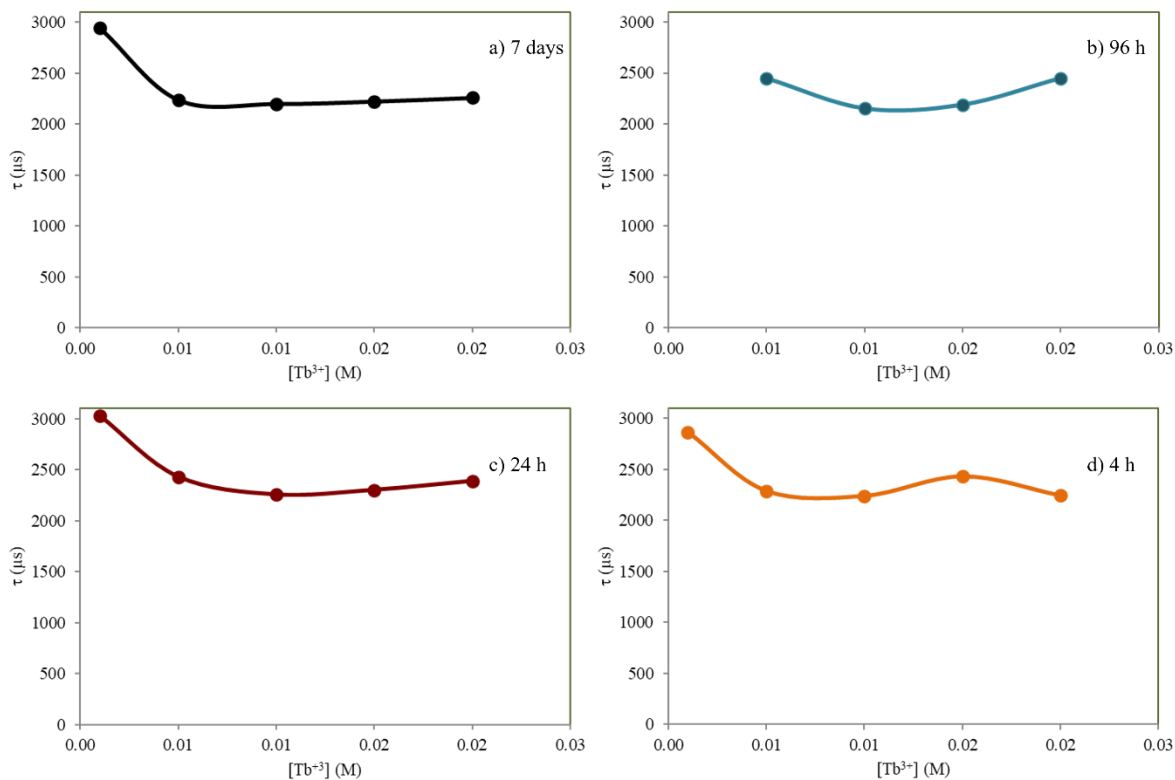


**Figure S12.** Variation of the luminescence lifetime in function of  $\text{Tb}^{3+}$  doping concentration of the  $\text{Tb}^{3+}$ :cit-cAp samples at several maturation times.

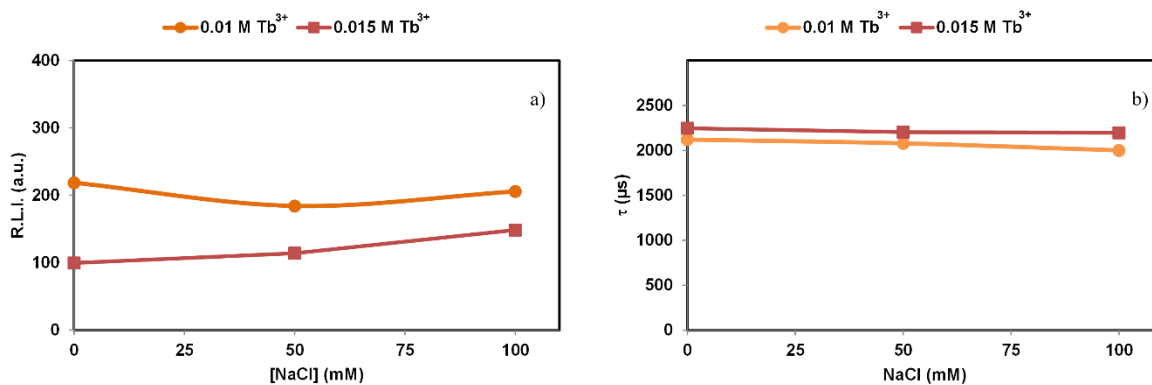


**Figure S13.** Effect of the ionic strength over the (a) R.L.I. and (b) luminescence lifetime of the  $\text{Tb}^{3+}$ :cit-cAp samples prepared with different  $\text{Tb}^{3+}$  doping concentrations at 96 h maturation time dispersed in aqueous media.

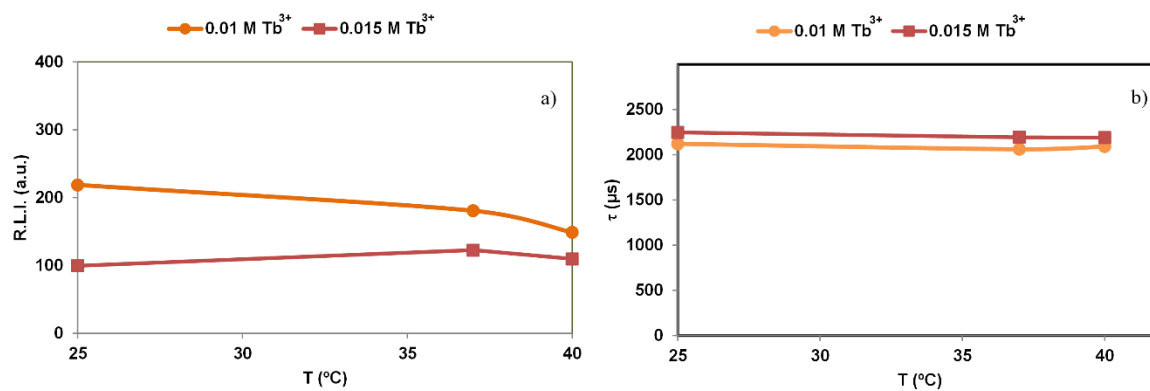


**Figure S14.** Effect of the temperature over the (a) R.L.I. and (b) luminescence lifetime of the Tb<sup>3+</sup>:cit-cAp samples prepared with different Tb<sup>3+</sup> doping concentrations at 96 h maturation time dispersed in aqueous media.